Available online at www.sciencedirect.com
SCIENCE DIRECT®
ELSEVIER
Journal of Magnetism and Magnetic Materials 256 (2003) 93–99
journal of magnetism and magnetic materials
www.elsevier.com/locate/jmmm

Magnetic properties of $Ni_{81}Fe_{19}/W_{90}Ti_{10}$ multilayers

M.A. Morales[a,*], H. Lassri[b], A. Biondo[a,c], A.M. Rossi[a], E. Baggio-Saitovitch[a]

[a] *Centro Brasileiro de Pesquisas Físicas, Rua Dr. Xavier Sigaud 150-Botafogo, 22290-180, Urca, RJ, Brazil*
[b] *Laboratoire de Physique des Matériaux et de Micro-électronique, Faculté des Sciences Ain Chock, Université Hassan II, B.P. 5366 Mâarif, Route d'El Jadida, Km-8, Casablanca, Morocco*
[c] *Departamento de Física, Universidade Federal do Espírito Santo, CCE-Campus de Goiabeiras 291060-900, Vitória, ES, Brazil*

Received 24 July 2001; received in revised form 13 May 2002

Abstract

The magnetization and anisotropy of $Ni_{81}Fe_{19}/W_{90}Ti_{10}$ multilayers prepared by DC sputtering are presented. At high-angle X-ray diffraction, weak superlattice peaks appear around the NiFe (1 1 1) diffraction line, which indicate a fiber texture $\langle 1\,1\,1 \rangle$ for NiFe. The magnetization decreases with NiFe layer thickness t_{NiFe} and the analysis of the results at 300 K indicates the presence of 6 Å thick dead $Ni_{81}Fe_{19}$ layer. The ferromagnetic resonance (FMR) spectra are obtained with the applied magnetic field parallel and perpendicular to the film plane at 300 K. Complicated spin-wave resonance spectra were observed and analyzed. From FMR, a negative value for $Ni_{81}Fe_{19}/W_{90}Ti_{10}$ interface anisotropy is obtained.

PACS: 75.70

Keywords: Permalloy; Ferromagnetic resonance; Multilayers

1. Introduction

Magnetic multilayered thin films with artificial periodicity (modulated structure) have attracted much attention in recent years due to their anomalous magnetic properties, such as changes in magnetization with the reduction of magnetic layer thickness, appearance, in some cases, of an uniaxial interfacial anisotropy, and interlayer exchange coupling [1–6]. These phenomena are commonly attributed to the existence of surface and interface states, e.g., the reduced coordination number and symmetry of atoms on the surface, transitional structure sublayers, and the availability and role of highly localized interfaces. As the dimensions decrease, the structures of the films became increasingly sensitive to the thickness of each constituent.

Permalloy ($Ni_{81}Fe_{19}$) heterostructures have great interest for magnetoresistive devices based on anomalous antiferromagnetic (AF)-coupling and giant magnetoresistance (GMR) in $Ni_{81}Fe_{19}$/Cu multilayers (MLs) [7–8] and spin-valves [8]. The AF-coupling and GMR depend sensitively on $Ni_{81}Fe_{19}$/Cu interface structure and the film morphology. The growth of epitaxial magnetic films and the effects of coherence strain on magnetic properties especially anisotropy and

*Corresponding author. Tel.: +55-21-2586-7150; fax: +55-21-2586-7540.
E-mail address: morales@cbpf.br (M.A. Morales).

0304-8853/03/$ - see front matter
PII: S0304-8853(02)00386-4

magnetic moment have been the object of many previous investigation [9]. However, unlike Ni and Fe, $Ni_{81}Fe_{19}$ possesses very little magnetocrystalline anisotropy and the primary source of anisotropy is uniaxial anisotropy induced during deposition.

Recently, ferromagnetic resonance (FMR) and spin-wave resonance (SWR) have been used to study the effective parameters of MLs, such as A_{eff} (the effective stiffness constant), $4\pi M_{\text{eff}}$ (effective magnetization), etc. [10–16]. In ML systems, the resonance condition and behavior might be more complicated than those in single-layer films, increasing the difficulty and uncertainly interpreting the FMR data.

In this paper, we present, the structural characteristics and the magnetic behavior of sputtered $Ni_{81}Fe_{19}/W_{90}Ti_{10}$ MLs with various thicknesses of $Ni_{81}Fe_{19}$ and $W_{90}Ti_{10}$ layers.

2. Experimental

The MLs were deposited onto water-cooled Si(1 0 0) substrates by dc sputtering. The chamber was initially evacuated to a pressure of 1–2×10^{-7} Torr, using a turbomolecular pump, argon of 5 N purity was used as the sputter gas keeping a constant pressure of 6×10^{-3} Torr in the chamber. Growth rates for NiFe and WTi were, respectively, 1.4 and 0.7 Å/s (these rates were obtained from X-ray reflectivity measurement on single films grown for different time intervals). In one series the magnetic layer thickness t_{NiFe} was varied in the range 10–100 Å and that of WTi layer t_{WTi} was fixed at 20 Å. In a second series t_{NiFe} was fixed at 40 Å and t_{WTi} was varied in the range 3–35 Å. The number N of bilayers were in the range 15–25 and all the samples were grown on 100 Å thick WTi buffer layer. In all cases the first and the last layer was WTi. In what follows the growth parameters of the samples will be indicated as $(t_{\text{NiFe}}/t_{\text{WTi}})_N$.

Low-angle X-ray diffraction (XRD) studies were made to check the periodic structure and to determine the layer thickness. Low-angle XRD of all the samples revealed peaks typical of the modulated structure and the thickness calculated from these peaks agrees with that designated according to the deposition rates. Magnetization M_S was measured using a vibrating sample magnetometer (VSM) with a precision better than $\pm5\%$ under magnetic fields up to 12 kOe. The magnetoresistance (MR) was measured using standard four-probe method with an applied field parallel to current in the film plane. The MR ratio is defined as $\Delta R/R=(R_0-R_S)/R_S$, R_S is the film resistance in saturation state in the applied field and R_0 in demagnetized state, respectively. All the measurements were carried out at room temperature.

The FMR spectra at 9.8 GHz, using a Bruker EPR spectrometer, were carried out, with the static field applied both perpendicular ($H_\perp$) and parallel ($H_\parallel$) to the film plane. We calculated the effective magnetization $4\pi M_{\text{eff}}=4\pi M_S-H_K$ where H_K is the perpendicular anisotropy field.

3. Results and discussion

The XRD pattern of $\theta-2\theta$ scan on the (NiFe 40 Å/WTi25 Å)$_{20}$ and (NiFe50 Å/WTi20 Å)$_{20}$ MLs is shown in Fig. 1. In the high-angle region, a broad peak close to the position expected for NiFe (1 1 1) appears. This is in agreement with texture measurements which indicate a $\langle 1\,1\,1\rangle$ fiber texture for NiFe. On each side of the NiFe (1 1 1) reflection from the ML there is a satellite peak, which is an evidence that coherent stacking exists in the ML. If coherent stacking did not exist, these high-angle satellite reflections would be absent [17]. However, these high-angle satellite peaks cannot be clearly observed with increasing NiFe layer thickness above than 35 Å and when decreasing the WTi thickness below than 7 Å, see Fig. 2. This result indicates that the coherent stacking cannot be maintained for the layer modulation wavelengths of NiFe/WTi MLs because of the large lattice mismatch between the NiFe and WTi. In the low-angle region, many peaks can be observed. Together with the satellite peaks in the high-angle region, this fact shows that the ML has a periodic structure. The period deduced from the low-angle Bragg peaks and the

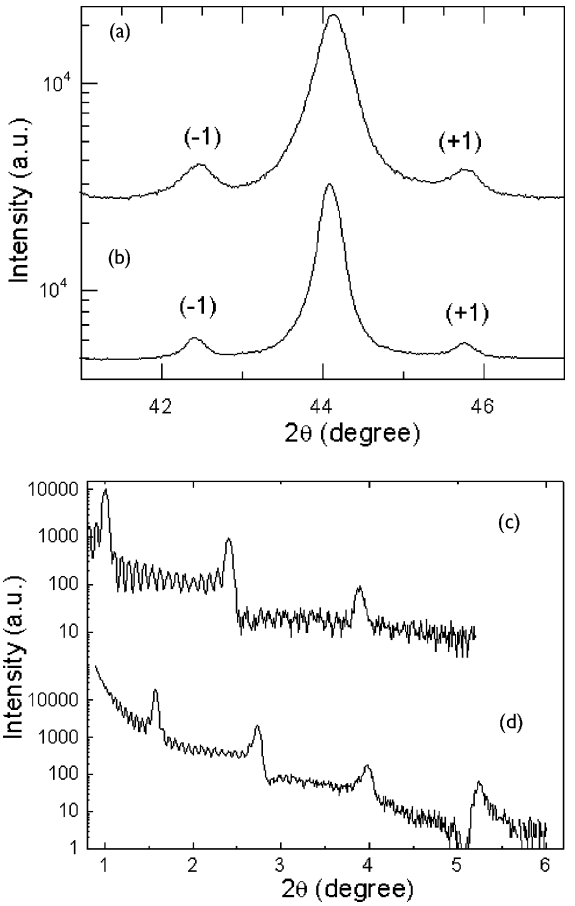

Fig. 1. Low-angle (a), (b) and high-angle (c), (d) X-ray diffraction patterns of (NiFe40 Å/WTi25 Å)$_{20}$ and (NiFe50 Å/WTi20 Å)$_{20}$ multilayers, respectively.

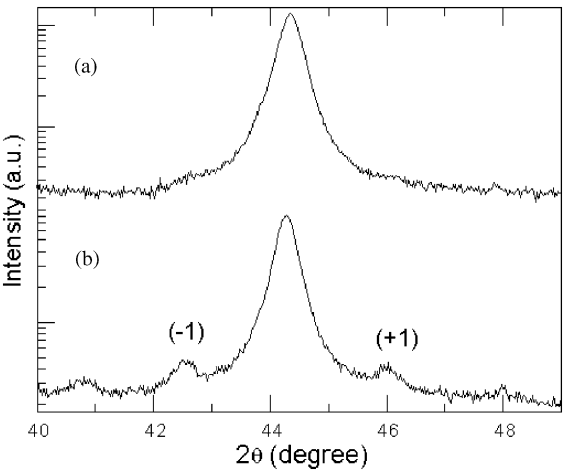

Fig. 2. High-angle X-ray diffraction patterns of: (a) (NiFe40 Å/WTi5 Å)$_{20}$ and (b) (NiFe40 Å/WTi9 Å)$_{20}$ multilayers.

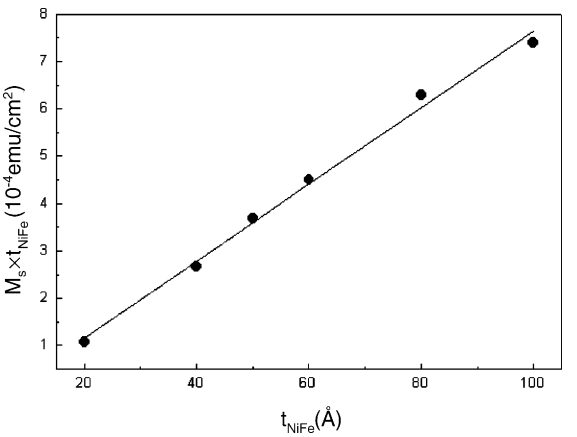

Fig. 3. The t_{NiFe} dependence of the product $M \times t_{NiFe}$ at 300 K.

satellite peak is in good agreement with the designated one.

The magnetization decreases with the decrease in NiFe layer thickness. This could be explained in terms of a magnetically dead layer of NiFe at each interface due to alloying effects. It is known from the dead layer model that the magnetization of multilayer (M) can be expressed

$$M = M_0(1 - t_0/t_{NiFe}), \quad (1)$$

where M_0 is the bulk NiFe value and $t_0/2$ is the dead layer thickness at each interface. The thickness of such a dead layer can be estimated as shown in Fig. 3, where we have plotted the product $M \times t_{NiFe}$ as a function of t_{NiFe}. The slope which corresponds to the magnetization yields 800 emu/cm^3. The intercept on the abscissa gives the value of t_0 which is found to be 6.0 ± 0.5 Å at 300 K.

Fig. 4 describes the variation of the MR with the magnetic layer thickness for NiFe/WTi MLs with a fixed nonmagnetic spacer layer thickness ($t_{WTi} = 20$ Å). The MR ratio displays a maximum of 0.8% at $t_{NiFe} = 50$ Å. The MR as a function of t_{WTi} is given in Fig. 5 where two defined oscillation peaks are evident: the first at $t_{WTi} = 13$ Å is quite narrow, while the second at 25 Å is broader. These

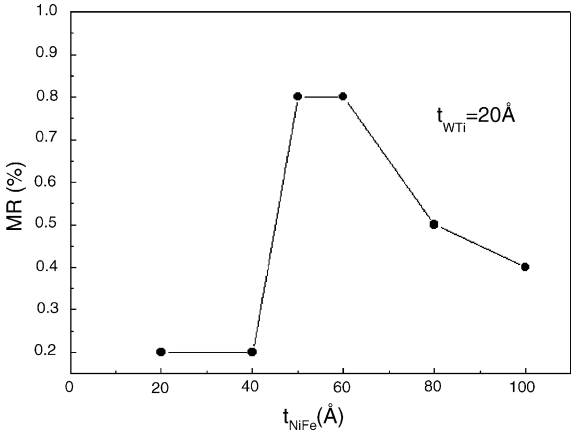

Fig. 4. MR ratio as a function of t_{FeNi} for $Ni_{81}Fe_{19}/W_{90}Ti_{10}$ multilayers.

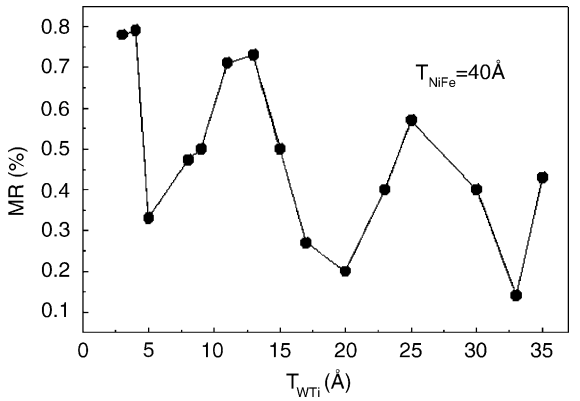

Fig. 5. Magnetoresistance curves of $Ni_{81}Fe_{19}/W_{90}Ti_{10}$ multilayers for different WTi layer thickness.

variations, which we assume correspond to the oscillation of the coupling between the NiFe layers from ferromagnetic to AF.

In the FMR spectra, the absorption line with maximum intensity is the uniform mode, corresponding to the regular in-phase excitation of the magnetization in NiFe/WTi MLs. When the magnetic field was parallel to the film plane, only one resonance peak related to the uniform mode appeared. When the field was applied perpendicular to the film plane, multiples resonance peak spectra were observed for the samples with $t_{NiFe} = 100$ Å, but only one or two peaks for $t_{NiFe} < 100$ Å. Fig. 6 shows two typical examples when $t_{NiFe} = 40$ and 100 Å. We have considered only the strongest mode to calculate $4\pi M_{eff}$ and the g factor. The g factor value for all the samples lies in the range 2.08–2.1, in agreement with the classical value of 2.09 for permalloy [18].

For $t_{NiFe} = 100$ Å, we observed spin-wave modes. Fig. 7 shows the dependence of the spin-wave resonance fields H_{res} on spin-wave number n in perpendicular geometry of (NiFe100 Å/WTi20 - Å) multilayer. This plot exhibits a linear relationship with respect to n when $n < 5$, as shown in the inset of Fig. 7, while a n^2 law holds when $n > 5$, n takes both odd and even numbers. In approximation, for high mode n, the n^2 law can be satisfied. This may be due the spin-waves modes that are pinned by a region of reduced magnetization and it is nonuniform within the magnetic sublayers, which is caused by alloying effect in NiFe/WTi MLs. The volume inhomogeneity model proposed by Portis [19] is likely suitable to describe the complicated dependence of spin-wave resonance fields H_{res}.

The effective anisotropy was deduced by using the following expressions where the resonance field H_{res} corresponds to the main mode:

For the perpendicular geometry we have

$$(\omega/\gamma)_{\perp} = H_{\perp} - 4\pi M_{eff}. \quad (2)$$

For parallel geometry we get

$$(\omega/\gamma)^2_{\parallel} = H_{\parallel}(H_{\parallel} + 4\pi M_{eff}). \quad (3)$$

As displayed in Table 1, the $4\pi M_{eff}$ and the linewidth $\Delta H_{\parallel}$ in the parallel geometry of NiFe/WTi MLs change in a correlated way. With increasing t_{NiFe} the effective magnetization increases and the linewidth decreases, respectively.

According to previous studies [1,20], an interface magnetic anisotropy of MLs can be deduced through the dependence of the perpendicular anisotropy on the thickness of the magnetic layer, if the interface anisotropy essentially enhances the first-order anisotropy energy K_1.

Then the perpendicular anisotropy field (excluding the demagnetization term) can be written as

$$H_K = H_U + 2H_S/t_{NiFe}, \quad (4)$$

i.e.

$$H_K = 4\pi M_S - 4\pi M_{eff}. \quad (5)$$

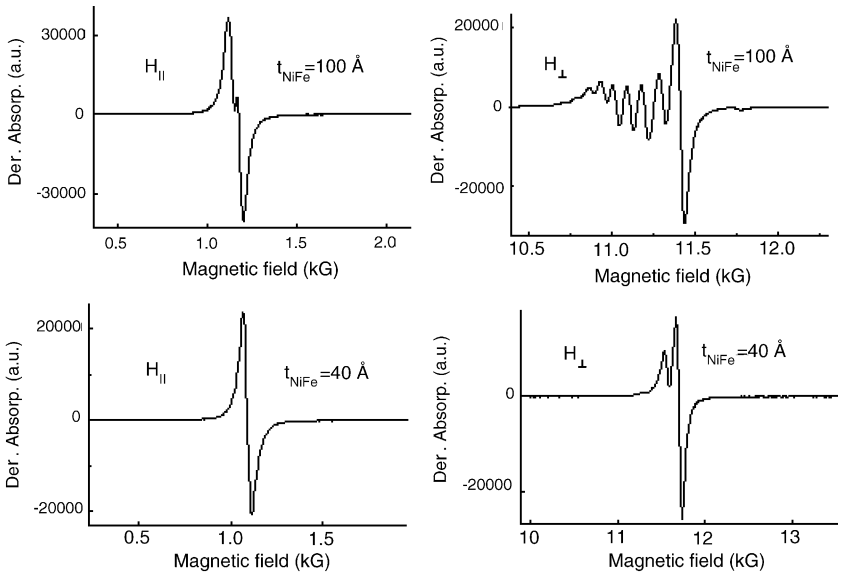

Fig. 6. FMR spectra with H perpendicular ($\perp$) and parallel ($\|$) to the film plane, for $Ni_{81}Fe_{19}/W_{90}Ti_{10}$ multilayers with $t_{NiFe} = 40$, and 100 Å, at $T = 300$ K.

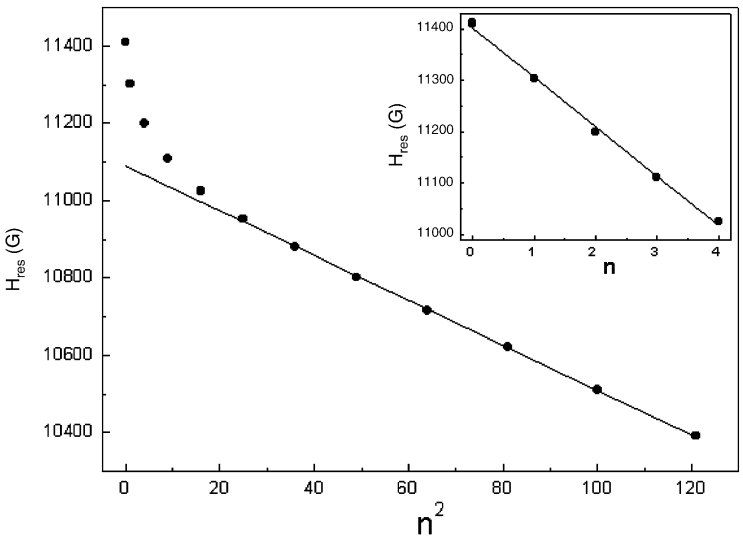

Fig. 7. Wave number n dependence of H_{res} for NiFe/WTi multilayer (with $t_{NiFe} = 100$ Å).

The perpendicular anisotropy field $H_K = 2K_1/M_S$ includes two terms, a volume anisotropy $H_U = 2K_U/M_S$, and a surface-induced one $H_S = 2K_S/M_S$.

Thus Eq. (4) can be written as

$$K_{eff} = K_V + 2K_S/t_{NiFe}, \tag{6}$$

where

$$K_{eff} = K_1 - 2\pi M_S^2, \quad K_V = K_U - 2\pi M_S^2. \tag{7}$$

K_{eff} and K_V are the effective perpendicular anisotropy energy and effective volume anisotropy energy, respectively (including the demagnetization energy). Fig. 8 shows a linear plot of H_K as a

Table 1
Summary of magnetic parameters on NiFe/WTi multilayers

t_{NiFe} (Å)	$4\pi M_S$ (G)	$4\pi M_{eff}$ (G)	$\Delta H_{\parallel}$ (G)
20	6707	7137	75
40	8340	8482	47
50	9232	9000	41
60	9420	8919	39
80	9885	9050	41
100	9294	8166	35

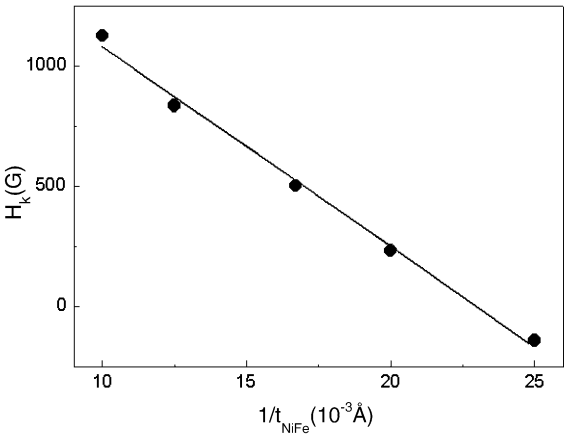

Fig. 8. Variation of H_K versus $1/t_{NiFe}$ for NiFe/WTi multilayers at 300 K.

function of $1/t_{NiFe}$ for the MLs with different NiFe layer thickness and a constant WTi layer thickness ($t_{WTi} = 20$ Å). From the slope of the straight line, the value of the interface anisotropy constant K_S is deduced to be $K_S = -0.17\,erg/cm^2$. Also, by extrapolating the straight line to $1/t_{NiFe} = 0$, we obtained $H_U = 1912$ Oe ($K_U = 0.76\times10^6\,erg/cm^3$).

In general, we assume that the surface anisotropy energy constant K_S could be treated as originated from several effects which change the surface spins at the interfaces such as misfit strain anisotropy [2], surface roughness [21–22] and Néel's anisotropy [23]. When there is some interdiffusion between the magnetic and nonmagnetic layers, roughness effects may strongly modify the magnetic surface anisotropy. Here K_S is a negative value, which means that the interface anisotropy confines the magnetization to the plane of the film. Furthermore, the anisotropy energy K_U (excluding the demagnetization energy) is much larger than the magnetocrystalline anisotropy energy of cubic NiFe. Assuming that a possible contribution to K_U arises from the effect of stress through magnetostriction.

4. Conclusion

In conclusion we have presented the ferromagnetic resonance (FMR) results for NiFe/WTi multilayers (MLs) prepared by DC sputtering. The magnetic anisotropy of the NiFe/WTi MLs has been investigated by FMR measurements. A negative interface anisotropy constant confines the magnetization to the plane of the film.

Acknowledgements

This work has been supported by CNPq and FAPERJ, H. Lassri thanks CBPF/MCT for the visitor fellowship, and thanks A.Y. Takeuchi for the support in the VSM measurements.

References

[1] U. Gradmann, J. Magn. Magn. Mater. 54–57 (1986) 733.
[2] F.J.A. den Broeder, W. Hoving, P.J.H. Bloemen, J. Magn. Magn. Mater. 93 (1991) 562.
[3] F.J.A. den Broeder, D. Kuiper, A.P. Van de Mosselaer, W. Hoving, Phys. Rev. Lett. 60 (1988) 2769.
[4] A.J. Freeman, R.W., J. Magn. Magn. Mater. 104–107 (1992) 1.
[5] R. Krishnan, H. Lassri, S. Prasad, M. Porte, M. Tessier, J. Appl. Phys. 73 (1993) 6433.
[6] S.S. Parkin, Appl. Phys. Lett. 58 (1991) 1473.
[7] S.S. Parkin, Appl. Phys. Lett. 60 (1992) 512.
[8] B. Dieny, V.S. Speriousu, B.A. Gurney, S.S. Parkin, D.R. Wilhoit, K.P. Roche, S. Metin, D.T. Peterson, S. Nadimi, J. Magn. Magn. Mater. 93 (1991) 101.
[9] A.F. Mayadas, M. Shatzkes, Phys. Ver. B 1 (1970) 1382.
[10] Z.J. Wang, S. Mitsudo, K. Watanabe, S. Awaji, K. Saito, H. Fujimori, M. Motokawa, J. Magn. Magn. Mater. 176 (1997) 127.

[11] J. Du, J. Wu, L.N. Tong, M. Lu, J.H. Du, M.H. Pan, H.R. Zhai, H. Xia, Phys. Status Solidi A 167 (1998) 183.
[12] H.R. Zhai, X.B. Zhu, M. Lu, Q.S. Bie, Y.B. Xu, Y. Zhai, Q.Y. Jin, M. Jimbo, S. Tsunashima, J. Magn. Magn. Mater. 140–144 (1995) 525.
[13] J. Du, M. Lu, L.N. Tong, W. Ji, H.R. Zhai, H. Xia, J. Magn. Magn. Mater. 177–181 (1998) 1209.
[14] N.K. Flevaris, R. Krishnan, J. Magn. Magn. Mater. 93 (1991) 439.
[15] R. Kordecki, R. Meckenstocck, J. Pelzl, E. Becker, G. Dumpich, G. Suran, J. Magn. Magn. Mater. 93 (1991) 281.
[16] H. Kubota, M. Sato, T. Miyazaki, Phys. Rev. B (52) (1995) 343.
[17] S.S. Jiang, J. Zou, D.J.H. Cockayane, A. Sikorski, A. Hu, R.W. Peng, Phys. Status Solidi A 130 (1992) 373.
[18] P. Djemia, F. Ganot, P. Moch, J. Magn. Magn. Mater. 165 (1997) 428.
[19] A.M. Portis, Appl. Phys. Lett. 2 (1963) 69.
[20] G.T. Rado, Phys. Rev. B 26 (1982) 295.
[21] P. Bruno, J. Appl. Phys. 64 (1988) 3153.
[22] P. Bruno, J. Phys. F 18 (1988) 1291.
[23] L. Néel, J. Phys. Radiat. 15 (1954) 225.